Characterization of a 95 kDa High Affinity Human High Density Lipoprotein-Binding Protein†

Alexander V. Bocharov,*,‡ Tatiana G. Vishnyakova,§ Irina N. Baranova,§ Amy P. Patterson,§ and Thomas L. Eggerman‡

Center for Biologics Evaluation and Research, Division of Cellular and Gene Therapy, Food and Drug Administration, 8800 Rockville Pike, Bethesda, Maryland 20892, and National Heart, Lung and Blood Institute, National Institutes of Health, 8800 Rockville Pike, Bethesda, Maryland 20892

Received June 30, 2000; Revised Manuscript Received January 30, 2001

ABSTRACT: A new human 95 kDa high density lipoprotein (HDL)-binding protein (HBP) corresponding to a high affinity HDL-binding site with $K_d = 1.67$ μg/mL and a capacity of 13.4 ng/mg was identified in human fetal hepatocytes. The HDL binding with the 95 kDa HBP plateaus at 2.5−5 μg/mL under reducing and nonreducing conditions. The association of HDL_3 with the 95 kDa HBP plateaued in 15−30 min while dissociation was complete in 30 min. HDL_3, apoA-I, and apoA-II were recognized by the 95 kDa HBP while low density lipoproteins (LDL) and tetranitromethane-modified HDL were not. The 95 kDa HBP predominantly resides on the surface of cells since trypsin treatment of HepG2 cells eliminated nearly 70% of HDL binding. All studied human cells and cell lines (HepG2, Caco-2, HeLa, fibroblasts, SKOV-3, PA-I) demonstrated the presence of the 95 kDa protein. Both RT-PCR and Western blotting for HB-2/ALCAM were negative in human fetal hepatocytes while Gp96/GRP94 was clearly differentiated from the 95 kDa HBP by two-dimensional electrophoretic mobility. Moreover, deglycosylation of HepG2 membrane preparations did not affect either HDL binding to the 95 kDa HBP or its size, while in contrast it affected the molecular weights of HB-2/ALCAM and SR-BI/CLA-1. We conclude that the 95 kDa HBP is a new HDL receptor candidate widely expressed in human cells and cell lines.

High density lipoproteins (HDL)[1] have been proposed as mediators of reverse cholesterol transport, removing cholesterol from peripheral tissues to the liver for metabolism (*1*). Both the efflux of cholesterol from cells to HDL and cholesterol ester (CE) uptake by liver cells as well as other HDL-related events in the cells have been proposed to be a result of HDL binding to cell surface HDL receptors (*2*). Indeed, overexpression of the HDL receptor (SR-BI or its human analogue CLA-1) has been reported to be associated with increased HDL binding (*3*, *4*). Additionally, both cholesterol efflux and selective cholesterol ester uptake were blocked by an anti-SR-BI antibody that attenuated HDL binding to SR-BI-overexpressing cells (*5*, *6*). Another membrane protein, ABCA-1, is an ATP cassette transporter that mediates cellular cholesterol pumping to plasma membrane (*7*). It has been reported to bind lipid-free apoA-I, but not HDL (*8*, *9*).

The Scatchard analyses of specific ^{125}I-HDL_3 binding to several cell types demonstrate the existence of two families of HDL-binding sites (*10*−*12*). A high affinity family (R1-HBS) has been reported to have K_d's of 0.4-2 μg/mL and a capacity of 10−40 ng/mg of cell protein while a lower affinity family (R2-HBS) has been reported to have K_d's of 20-40 μg/mL and a capacity of 100−1000 ng/mg of cell protein. In addition to the physiologically relevant SR-BI and ABCA-1, several other HDL-binding proteins have been cloned including HBP, HB-2, and GRP94, and their role in HDL metabolism is under investigation (*13*−*15*). The contribution of these HBP's as well as the physiologically relevant SR-BI and ABCA-1 to cellular HDL binding in normal cells is uncertain; however, when these proteins were overexpressed, the increased association of iodinated HDL has been reported to impact the lower affinity HDL-binding sites rather than the higher affinity sites (*3*, *14*, *15*).

Unlike the R2-HBS family, for which SR-BI is an example, the physiological role of R1-HBS remains to be determined. It has been suggested (*16*) that R1-HBS may participate in the uptake and the internalization of remnant HDL generated by hepatic lipase. The R1-HBS may also impact HDL retroendocytosis observed in epithelial cells and macrophages (*17*, *18*). In contrast to the lower affinity family, the R1-HBS demonstrates high ligand association and dissociation rates (*10*−*12*), the latter of which makes it difficult to detect the corresponding HBP(s) by conventional methods such as HDL−ligand blotting.

The aim of this study was to identify and characterize high affinity HDL-binding protein(s) by a modified ligand blotting

† A.V.B. was a participant of the Research Scholar Program sponsored by CBER/FDA USA under administration by the Oak Ridge Institute for Science and Education.

* Correspondence should be addressed to this author at the Division of Cellular and Gene Therapy, Food and Drug Administration, CBER/OTRR, 8800 Rockville Pike, NIH Campus Building 29B, Room 2NN12, Bethesda, MD 20892. Tel: (301) 827-0692; Fax: (301) 827-0449; E-mail: bocharov@cber.fda.gov.

‡ Food and Drug Administration.

§ National Heart, Lung and Blood Institute.

[1] Abbreviations: HDL, high density lipoprotein; HBP, high density lipoprotein-binding protein; apoA-I, apolipoprotein A-I; apoA-II, apolipoprotein A-II; HBS, high density lipoprotein-binding site; SR-BI, scavenger receptor B-I; HB-2, high density lipoprotein-binding protein 2.

10.1021/bi001503k CCC: $20.00
Published on Web 03/15/2001

method, which would potentially allow the demonstration of HBP(s) characterized by a rapid dissociation rate. The usual ligand blotting procedure was redesigned by shortening the washing step followed by fixing with paraformaldehyde. The sensitivity of ligand blotting was also increased by using immunodetection of bound ligand with specific antibodies against HDL apolipoproteins. Using these modifications, we have identified a human 95 kDa HDL-binding protein whose HDL-binding properties resemble a R1-HBS.

MATERIALS AND METHODS

HDL_3: Isolation and Iodination. Human HDL_3 ($1.125 < d < 1.216$) was isolated from plasma of healthy donors by two repetitive centrifugations by the method of Redgrave (*19*). The HDL_3 were passed through an agarose−heparin column (HiTrap, Amersham Pharmacia Biotech), and an apoE-free HDL_3 fraction was collected. Labeling of HDL_3 with $Na^{125}I$ was performed by the *N*-bromosuccinimide method according to Sinn et al. (*20*). The specific radioactivities ranged from 1000 to 3000 cpm/ng of protein with more than 98% of the radioactivity being protein-associated.

Hepatocyte Isolation and Culture. Fetal tissues were obtained from normal elective or spontaneous pregnancy terminations. The use of these tissues was approved by the Institutional Review Board of the Cardiology Research Center and the Russian Ministry of Health (no. 947, 1983). No tissues were harvested from cases associated with intrauterine death or known fetal abnormalities.

Liver cells were prepared using a two-step collagenase perfusion technique (*21*−*23*). Briefly, liver (20−40 g) was perfused through the portal vein by 400 mL of 37 °C Ca^{2+}/Mg^{2+}-free HBSS solution containing 5 mM EDTA, at a rate of 40 mL/min, followed by 100 mL of Ca^{2+}/Mg^{2+}-free HBSS solution w/o EDTA. Enzymatic treatment was performed with 1 mg/mL type IV (Sigma) collagenase in Mg^{2+}-free HBSS with 5 mM $CaCl_2$ for 20 min at the rate of 20 mL/min. Hepatocytes were separated by four low-speed centrifugations at 50*g* for 2 min each. Hepatocytes were further centrifuged in a 60% Percoll solution at 250*g* for 10 min. When pelleted, the resulting cells were determined to be more than 75% hepatocytes and have 98% viability as determined by trypan blue exclusion. Hepatocytes were plated on collagen-coated culture dishes [12-well Costar culture clusters or 90 (150) mm Petri dishes] at a density 1×10^5 cells/cm^2 in Williams' E medium (Sigma) containing 2 μg/mL insulin, 10^{-7} M dexamethasone, 100 μg/mL kanamycin, and 20 mM HEPES. The hepatocytes were allowed to attach for 2−3 h, and then the medium was replaced to remove unattached cells, which were mostly hepatic nonparenchymal cells. Subsequently, the medium was replaced daily. The cells maintained 98% viability for 8−9 days and demonstrated negligible release of cellular lactate dehydrogenase, a marker of plasma membrane integrity (*23*). During the study (1−9 days), the cells maintained typical epithelial morphology and had less than 5% of contaminating nonparenchymal cells (Figure 1A,B).

Cell Lines. HepG2 (human hepatocarcinoma), HeLa (human epitheloid carcinoma), PA-I (human prostate epitheloid carcinoma), SKOV-3 (human ovary epitheloid carcinoma), Caco-2 (adenocarcinoma, colon), and human fibroblasts were grown until 50−60% confluence in EMEM medium containing 10% FCS, and 100 μg/mL kanamycin. Subsequently, cells were washed to remove residual serum with PBS and further cultured in Williams' E medium containing 2 μg/mL insulin, 10^{-7} M dexamethasone, 100 μg/mL kanamycin, and 20 mM HEPES for a 3 day period. The medium was replaced daily, and the cells were subsequently used for plasma membrane preparations.

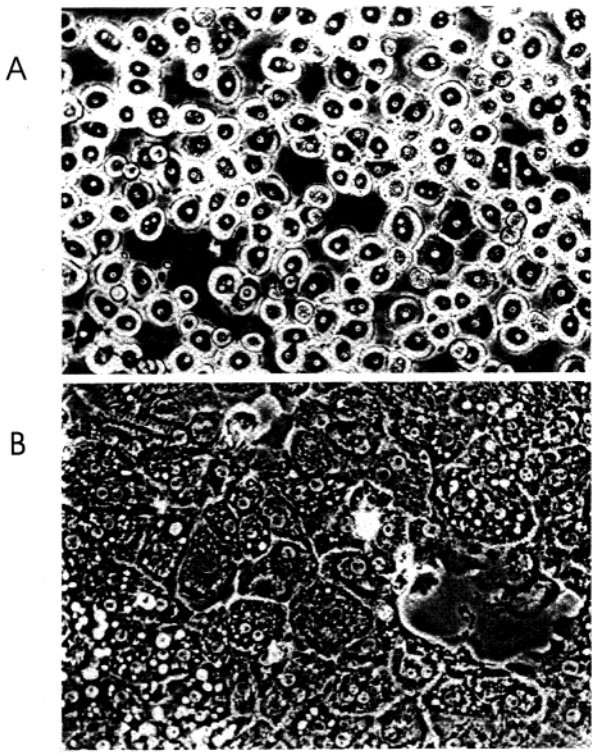

FIGURE 1: Phase contrast microscopy of cultured human fetal hepatocytes (×100). Panel A: 4 h after cell plating. Panel B: 48 h after cell plating.

Binding Assay. Saturation binding experiments were performed at 4 °C using ^{125}I-HDL_3 concentrations between 1.25 and 160 μg/mL. Hepatocyte monolayers cultured in Costar 12-well culture plates were washed 2 times with 2 mL of ice-cold HBSS and subsequently placed on ice. The cells were incubated with ice-cold HBSS containing 20 mg/mL BSA and labeled ligand in the presence or absence of 50-fold excess unlabeled HDL_3. After a 2 h incubation on ice, the cells were rinsed once with 6 mL of ice-cold HBSS. Cultured cells were further incubated with a Pronase/Dispase I (neutral proteases, Boehringer Mannheim) solution in HBSS (100 μg/mL of each) for 30 min at 4 °C in order to release surface-bound radioactivity as we reported previously (*23*). Radioactivity was counted in an LKB-Wallac Ultragamma counter. Specific binding was determined as the difference between total and nonspecific binding (the amount of radioactivity measured in the presence of 50×-fold excess unlabeled ligand). The protein content of samples was determined after hydrolysis in 0.1 N NaOH followed by neutralization with 0.1 N HCl using the method of Bradford with albumin as the standard (*24*).

Preparation of Liver Cell Membranes. All procedures were carried out on ice. Confluent monolayers of hepatocytes were washed 3 times with ice-cold 10 mM Tris-HCl (pH 8.0), 150 mM NaCl, 5 mM EDTA, and 1 mM phenylmethylsulfonyl fluoride, removed by scraping with a rubber policeman,

and then homogenized in 10 mM Tris-HCl (pH 8.0), 300 mM sucrose, 5 mM EDTA, and 1 mM phenylmethylsulfonyl fluoride using a Polytron homogenizer at 24 000 rpm for 20 s. The supernatant obtained by centrifugation at 10000*g* for 10 min was then centrifuged at 100000*g* for 60 min. The supernatant was then removed and used as a cell cytosol preparation; the pellet was resuspended and boiled in SDS−PAGE sample buffer and then analyzed in the ligand immunoblot assay.

Ligand Blot Assay for HDL-Binding Proteins. The regular ligand blot assay was performed as previously described (*25*). Samples of plasma membrane proteins were separated by 7.5% polyacrylamide SDS gel electrophoresis (SDS−PAGE) under nonreducing conditions utilizing a BioRad Mini-protean II electrophoresis cell (*26*). Separated proteins were electrophoretically transferred onto BA-83 nitrocellulose membranes (Schleicher & Schuell) for 1 h, 15 V, 8 °C. The nitrocellulose membranes/strips were incubated for 2 h with blocking buffer [10 mM Tris-HCl (pH 7.4), 150 mM NaCl, 5% (w/v) lipid-deficient (5 wt %/wt) low lipid milk powder] at room temperature. Subsequently, the strips were incubated for 30 min (or 24 h) with 0.625−40 μg/mL HDL_3 at 4 °C in blocking buffer. Then strips were washed 5 times for 3 min with blocking buffer. HDL_3−HBP complexes were visualized using mouse anti-human apoA-I monoclonal antibody 7C1 (gift of Mona Co., Russia) as the first antibody and sheep anti-mouse IgG antibodies conjugated with alkaline phosphatase absorbed with human plasma proteins (Sigma) as the second antibody.

To decrease the amount of dissociating receptor−HDL complexes during the washing step and detection, a modified ligand blotting protocol was used. After a single washing of membrane with 10 mL per strip (50 mL per whole 5 × 10 cm BA-83 membrane) of ice-cold blocking buffer w/o milk, proteins were fixed to the membrane by incubation with 4% paraformaldehyde in 100 mM phosphate buffer, pH 7.4, for 30 min at room temperature. Subsequently, the strips were washed 3 times with blocking buffer, and further processed as outlined above in the regular protocol. In the cases when apoA-I or apoA-II were used as the ligands, goat anti-human apoA-I or anti-apoA-II (Boehringer Mannheim) was utilized as a first antibody, and rabbit anti-goat IgG antibodies conjugated with alkaline phosphatase absorbed with human plasma proteins (Sigma) were used as the second antibody.

Trypsin Treatment of Cells and Subcellular Localization of the 95 kDa HBP. HepG2 cells were plated onto collagen-coated 24-well Costar multiwells. After becoming confluent, the cells were rinsed with PBS, pH 7.4, and treated with 0.5 mL 5× trypsin solution (Sigma, T-4174) or incubated with PBS, containing 5 mM EDTA (control), pH 7.4, for 30 min at 37 °C. Both control and trypsin-treated cells were collected and then washed 3 times with ice-cold PBS containing 1 mg/mL soybean trypsin inhibitor by three 50*g* centrifugations for 3 min each. The cells were used for crude plasma membrane and cellular cytosol as outlined above. Membrane preparations were extracted with 1% Triton X-100 in TBS, pH 7.4, precipitated with methanol, brought up in SDS−PAGE sample buffer, and boiled. Cytosol fractions were used for detection of β-actin by Western blotting utilizing monoclonal anti-β-actin clone AC-74 (Sigma A-5316). Both plasma membrane preparations and cytosol fractions were then analyzed by the modified HDL−ligand blot assay.

Ligand Immunoblot Assay for LDL-Binding Proteins. LDL at a concentration of 10 μg/mL was utilized instead of HDL_3 in the modified ligand blotting protocol described above. To visualize the ligand−receptor complexes, 5F8 mouse monoclonal anti-human LDL IgG (Gift of Mona Co., Russia) was used as a first antibody to detect the LDL-binding protein complexes followed by incubation with goat anti-mouse IgG conjugated with alkaline phosphatase (Sigma) as a second antibody.

Western Blotting. The same membrane preparations as used for the ligand immunoblotting experiments were used for Western blot analyses. After blocking in TBS (5% fat-free milk, pH 7.4), nitrocellulose membranes were incubated for 2 h at room temperature with mouse monoclonal anti-ALCAM/HB-2 (1:1000; RDI), or rabbit anti-SR-BI/CLA-1 (1:1500; Novus Biological) or rat monoclonal anti-GRP94 (1:400; NeoMarkers) antibodies in blocking buffer. After 5 × 3 min incubations with blocking buffer, alkaline phosphatase-conjugated anti-mouse, -rabbit, or -rat antibodies (all from Sigma) in blocking buffer at a dilution of 1:10 000 were incubated for 1 h at room temperature as second antibodies. Visualization was performed utilizing nitro blue tetrazolium/5-bromo-4-chloro-3-indolyl phosphate in 5 mM $MgCl_2$, 100 mM TRIS, pH 9.5.

Two-Dimensional Electrophoresis and HDL−Ligand Blotting. HDL-binding proteins were partially purified by preparative electrophoresis. Briefly, approximately 1 mg of HepG2 plasma membrane preparation was separated by 7.5% SDS−PAGE electrophoresis. The gel region between 80 and 120 kDa, as determined by SeeBlue prestained protein standards (Novex), was cut off, and the proteins were eluted from the gel using a model 422 electro-eluter (BioRad). Eluted proteins were concentrated by filtration on Microcon YM-30 filters (Amicon) and utilized for gradient 4−12% SDS−PAGE and two-dimensional electrophoresis.

Two-dimensional electrophoresis was performed according to the method of O'Farrell (*27*). Isoelectric focusing was carried out in a glass tube of inner diameter 1.0 mm using 2% pH 3.5−10 ampholines (Pharmacia Biotech) according to the BioRad manual. Approximately 5 μL (20 μg) of partially purified HDL-binding protein was mixed with 5 μL of IEF sample buffer (BioRad) and applied to the IEF gel. For the second dimension, a 7.5% SDS−PAGE gel was utilized. Proteins were electroblotted onto BA83 nitrocellulose (30 V, 18 h, 8 °C) and characterized by ligand blotting utilizing 50 μg/mL HDL. HDL binding was determined after 24 h of incubation at 4 °C. The other steps were performed according to the modified ligand blotting procedure as outlined above. In a separate experiment, BA-83-immobilized proteins were stained with goat anti-GRP94 antibodies. The mixture included anti-C-terminal (C-19) peptide and anti-N-terminal (N-19) peptide, each diluted at 1:1000 (Santa Cruz Biotechnology) or rat anti-GRP94 monoclonal antibody at a dilution of 1:500 (NeoMarkers). The same samples were analyzed by ligand blotting and anti-GRP94 Western blotting after gradient 4−12% SDS−PAGE under the conditions described for two-dimensional separation.

Tetranitromethane Treatment of HDL. HDL were modified with tetranitromethane (Sigma, T-5752) by incubating HDL with 3.0 and 10 mM tetranitromethane (TNM) as reported before (*28*). TNM-modified HDL was analyzed by a 12.5% SDS−PAGE and native 4−20% PAGE (Novex) gel elec-

Table 1: Upstream and Downstream Primers Used for Specific RT-PCR

lipoprotein binding protein	forward primer/reverse primer
HDL binding protein	5′-CATCTCTGCCGAGCACAAACG-3′ 5′-GGTCAAGCTATTGGCCTTGGCATAGAC-3′
HB-2	5′-GTATGATGATGTACCAGAGTACAAGG-3′ 5′-GGGACCCAACAAGTTCAAGTGTCACAGC-3′
CLA-1	5′-GAGCGTGGACCCTATGTCTACAGG-3′ 5′-CACAGTGAAGAGCCCAGAGTCTGAG-3′
ALCAM	5′-GTATGATGATGTACCAGAGTACAAGG-3′ 5′-GGTGAATGGCATTTGTATGTCAG-3′

trophoresis under nonreducing conditions. The ability to interact with HepG2 HBP(s) was analyzed by the modified ligand immunoblotting procedure as indicated above.

Deglycosylation of Plasma Membrane Protein Preparations by Digestion with Glycosidases. HepG2 cells were extracted for 5 min in TBS, pH 7.4, with 1% Triton X-100, and then incubated with a mixture of endo-β-*N*-acetylglucosaminidase F, *N*-glycosidase F, and endoglycosidase H at 5 units/mL of each at 37 °C for 45 min. In control preparations, extracts were incubated at the same temperature without addition of the enzymes. Both extracts were precipitated with methanol, solubilized with SDS−PAGE sample buffer, and applied to a 7.5% SDS−PAGE gel. After gel electrotransfer onto BA-83 nitrocellulose, the blots were used for modified ligand blotting with 10 μg/mL HDL_3 or for Western blotting analyses (see above).

RNA Isolation. Total RNA was extracted from cells or tissue homogenates by Trizol reagent (Gibco) following the manufacturer's instructions.

RT-PCR Analyses. The RNA from human fetal hepatocytes, human fetal liver, human adult liver, human fetal gut, McA-RH7777, and HepG2 cells was analyzed by using a RT-PCR assay based on the RNA PCR kit protocol supplied by Perkin-Elmer. The RT was done in a 30 μL volume, applying 2 μg of total RNA and 20 pmol of random primer (Boehringer Mannheim) at 37 °C for 60 min followed by 5 min at 95 °C. The subsequent PCR step was performed in a volume of 50 μL under optimized $MgCl_2$ concentrations and temperature conditions with 10 pmol of specific primer sets for 38 cycles. The cycle profile used on the Perkin-Elmer DNA Thermal Cycler 480 was 60 s at 94 °C, 60 s at TA (50−60 °C), and 60 s at 72 °C. The experiments were accompanied by water controls.

Primers for RT-PCR. The HBP, HB-2, ALCAM, and SR-BI specific primer pairs were derived from sequence data available in the scientific literature for HBP (*13*), HB-2 (*14*), ALCAM (*29*), and CLA-1 (*30*). Table 1 provides the specific primer sets.

Scatchard Analyses. Saturation curves were determined by measuring the amount of HDL_3 bound to nitrocellulose membrane in arbitrary units. The membranes, after the developing reaction, were scanned with a model SNAPScan 1236 scanner, and the intensities of stained bands were determined by a SigmaGel (Sigma) or Gel-Pro analyzer (Media Cybernetics). Specific binding of HDL_3 to a band was calculated as the density in the area of the band minus an average background determined by the software on the same membrane strip.

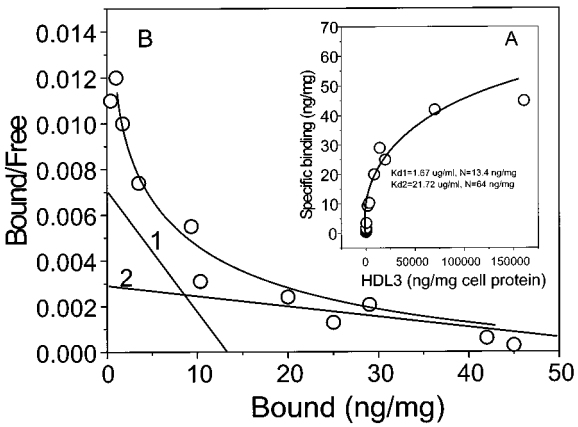

FIGURE 2: Binding of ^{125}I-HDL_3 to cultured human fetal hepatocytes. Hepatocytes were cultured for 48 h after plating, washed, and then incubated with increasing concentrations of ^{125}I-HDL_3 to obtain saturation binding data. The specific binding curve was obtained by subtracting the nonspecific binding data from the total binding data (panel A). Panel B: Scatchard transformation of the specific binding data. The solid lines represent the best-fit computer-generated lines, composed of high- (1) and low-affinity (2) sites. The data are the mean of triplicate determinations and are representative of four experiments.

Association and Dissociation Experiments. The association of 10 μg/mL HDL_3 was performed at 4 °C in blocking buffer. At specified time points, strips were washed with a single volume of ice-cold TBS, pH 7.4, and subsequently proceeded according to the modified ligand blot protocol.

Dissociation experiments were carried out at 4 °C after the initial association of 10 μg/mL HDL_3 with membrane strips for 30 min followed by a wash with a single volume (10 mL) of ice-cold TBS, pH 7.4. The dissociation was initialized by placing strips into 50 mL of blocking buffer. At specified times, strips were removed from the blocking buffer and washed with a single volume of ice-cold TBS (10 mL), pH 7.4, followed by fixing with 4% paraformaldehyde.

RESULTS

Saturation Binding Study. To evaluate HDL binding to cultured human fetal hepatocytes, HDL-binding studies were performed using a high specific activity ^{125}I-HDL_3 (3000 cpm/ng of protein) and the rapid washing protocol. The results of these experiments are seen in Figure 2A. The LIGAND program fitted the data to a two-site model significantly better than to a single-site model ($p < 0.01$). Scatchard transformation of the ^{125}I-HDL_3 binding data (Figure 2B) revealed more than one binding component, a R1-HBS ($K_d = 1.67$ μg/mL, $N = 13.4$ ng/mg of cell protein) and a R2-HBS ($K_d = 21.72$ μg/mL, $N = 64$ ng/mg of cell protein). When using the longer washing protocol, no R1-HBS was demonstrated whereas the R2-HBS binding was unaltered (data not shown). This agrees with previous data on both rat liver (*10*) and rat hepatocytes (*12*) which demonstrated two HDL-binding sites with relatively high (R1 $K_{d_1} = 1-2$ μg/mL) and low affinity (R2 $K_d = 20$ μg/mL) when utilizing a combination of high specific activity ^{125}I-HDL_3 and rapid removal of unbound ^{125}I-HDL_3.

Ligand Blotting Experiments. Cell-surface-specific HDL binding has been resolved into two types of HDL-binding components with different saturation binding parameters and

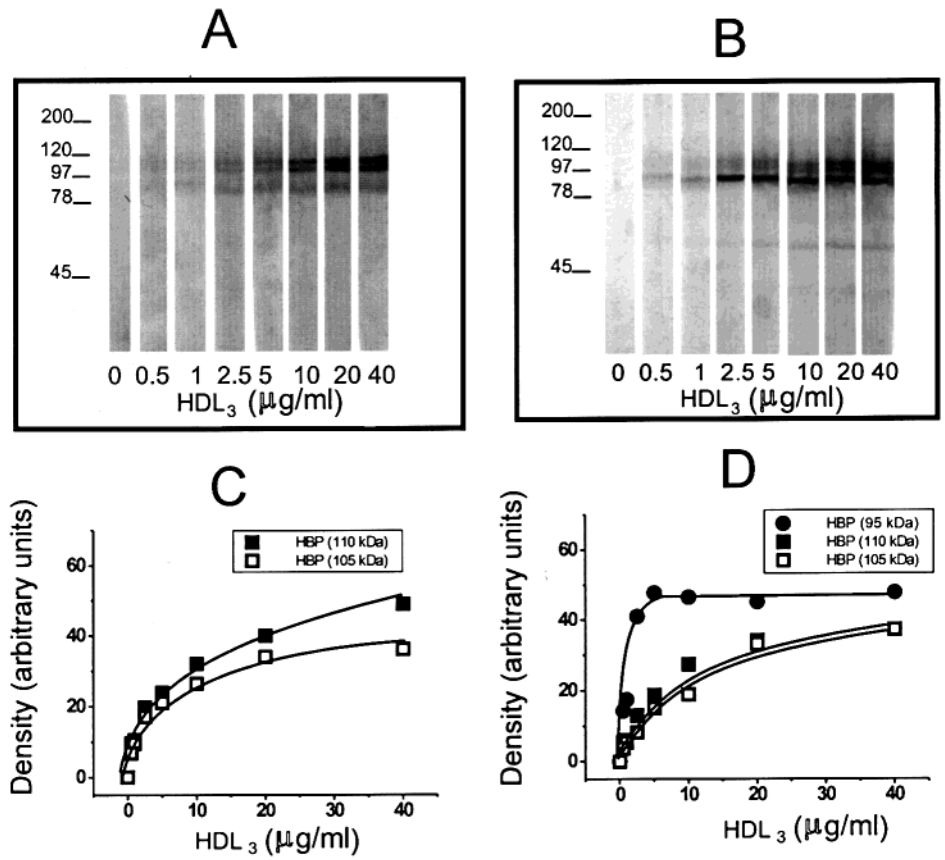

FIGURE 3: Concentration-dependent HDL_3 binding to fetal hepatic plasma membrane proteins using the regular and modified ligand blotting methods. The binding of various HDL_3 concentrations (24 h, 4 °C) was evaluated by either the regular ligand blotting protocol (panel A) or the modified protocol (panel B). After the nitrocellulose strips were scanned, the curves were generated by the SigmaGel computer program with panel C representing the data in panel A and panel D representing the data in panel B.

association/dissociation rates (*10*−*12*). Since R1-HBS was only observed with the rapid washing protocol, we modified the ligand blotting protocol by similarly decreasing the duration of the washing step to a single volume of ice-cold ligand-free solution. Additionally we fixed the receptor-bound HDL_3 with a 4% paraformaldehyde solution. Since incubations at room temperature and 37 °C demonstrated high background staining, all binding studies were performed at 4 °C. A comparison of the two ligand blotting methods for evaluating HDL_3 binding to a human fetal hepatocyte plasma membrane preparation during overnight association is seen in Figure 3. Two HBP's were detected in the 105−115 kDa region (Figure 3A) when the strips were incubated with HDL_3 at 4 °C overnight and utilizing the regular ligand immunoblotting method. The saturation HDL_3-binding curve demonstrates that these two HBP's plateaued at 20−25 μg/mL (Figure 3C). Similar saturation curves were previously observed with the specific binding of ^{125}I-HDL_3 to rat (*23*) when the regular washing procedure was used. This observation demonstrates that these HBP's may belong to the family of proteins displaying HDL-binding characteristics of R2-HBS. In addition to the two proteins observed with the regular washing procedure, a shorter washing time followed by paraformaldehyde fixing allowed a new HBP to be observed with a molecular mass of approximately 95 kDa (Figure 3B). In contrast to the 105−115 kDa HBP's, the binding of HDL_3 with the 95 kDa protein plateaued at a concentration of about 2.5−5 μg/mL (Figure 3D), demonstrating that this protein may belong to the family of R1-HBS.

HDL Association and Dissociation Kinetics. Binding time course experiments were undertaken to determine the kinetics of HDL_3 binding to the 95 kDa HBP. No HDL_3 binding could be detected with the 105−115 kDa proteins during the initial 180 min of incubation (Figure 4A) while HDL_3 binding with the 95 kDa protein reached approximately 90% of maximal binding by 15−30 min (Figure 4B). These data indicate that a short-term HDL_3 association (between 15 and 60 min) could selectively detect the 95 kDa HBP. A shorter differential time course of HDL_3 binding to the R1/R2 HBS's has been observed with ^{125}I-HDL_3 binding in HepG2 cells (*11*) and rat hepatocytes (*12*) A potential explanation for this difference is an alternative conformation of the 105−115 kDa HBP's when absorbed to the nitrocellulose membrane.

The dissociation of HDL_3 from the 95 kDa HBP/ HDL_3 complexes was studied after 30 min of association. Free ligand was then removed, and the strips were washed with a single volume of ice-cold ligand TBS buffer (10 mL), pH 7.4. Afterward, individual nitrocellulose strips were placed into 50 mL of blocking buffer and incubated on ice for the indicated time periods (Figure 4C). The 95 kDa HBP was observed as the only stained band on nitrocellulose strips after 30 min of association (Figure 4C). The dissociation of HDL_3 from the 95 kDa HBP was rapid (Figure 4D). By 15 min, approximately 90% of the initially bound HDL_3 dissociated (Figure 4E). By 30 min, the dissociation was complete.

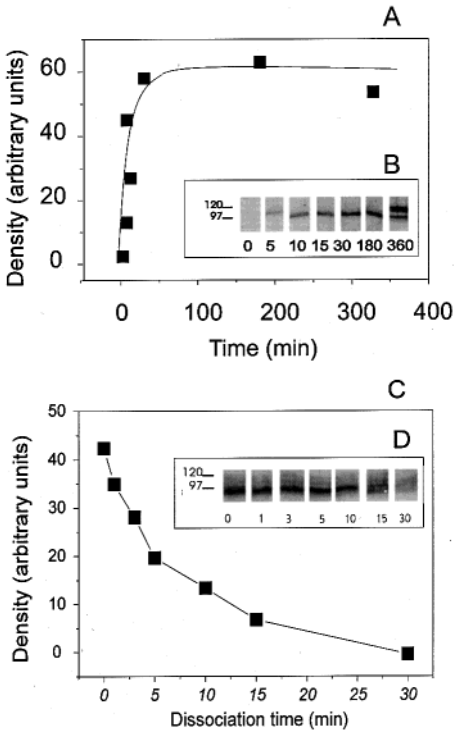

FIGURE 4: Time course of HDL_3 association and dissociation with the 95 kDa HBP. Panel A: The strips from panel B were scanned, and curves were generated using the SigmaGel computer program. Panel B: Nitrocellulose strips were incubated for the indicated times using 10 μg/mL HDL_3. Panel C: The strips from panel D were scanned, and curves were generated using the SigmaGel computer program. Panel D: Nitrocellulose membrane strips were incubated with HDL_3 at a concentration of 10 μg/mL for 30 min at 4 °C. After the association phase, the strips were incubated on ice in 50 mL of ligand-free blocking buffer for the indicated time (dissociation phase). The strips were then processed according to the modified ligand blotting protocol (see Materials and Methods).

Effect of Reducing Conditions on HDL_3 Binding with the 95 kDa HBP. For these experiments, fetal hepatocyte plasma membrane proteins were separated by PAGE under reducing and nonreducing conditions. Utilizing a 30 min association of HDL_3, the only protein observed was the 95 kDa HBP. The saturation binding curves were similar under reducing (Figure 5A,C) and nonreducing (Figure 5B,D) conditions, indicating that HDL_3 binding was unaffected by S−S bond reduction.

Ligand Specificity. Lipoprotein/apolipoprotein-binding experiments were conducted to study the ligand specificity of R1-HBP utilizing a 30 min incubation of HDL_3 (10 μg/mL), apoA-I (1 μg/mL), apoA-II (1 μg/mL), or LDL at a concentration of 10 μg/mL. After the initial association, following rapid washing and fixing, the ligand−receptor complexes were visualized with the anti-apoA-I 7C1 monoclonal antibody for HDL_3 and apoA-I binding, with rabbit anti-human apoA-II for apoA-II binding, or with monoclonal anti-apoB 5F8 as the antibody for LDL binding (Figure 6). HDL_3, lipid-poor apoA-I, and apoA-II all bound to the R1-HBP whereas they did not interact with 105−115 kDa HBP's. No binding of LDL was demonstrated with the 95 kDa HBP or the 105−115 kDa HBP's. In competitive binding experiments, using LDL concentrations up to 400 μg/mL, LDL did not compete with HDL_3 (10 μg/mL) binding for the R1-HBP (Figure 6). In contrast, a significant competition of LDL (400 μg/mL) was observed with the

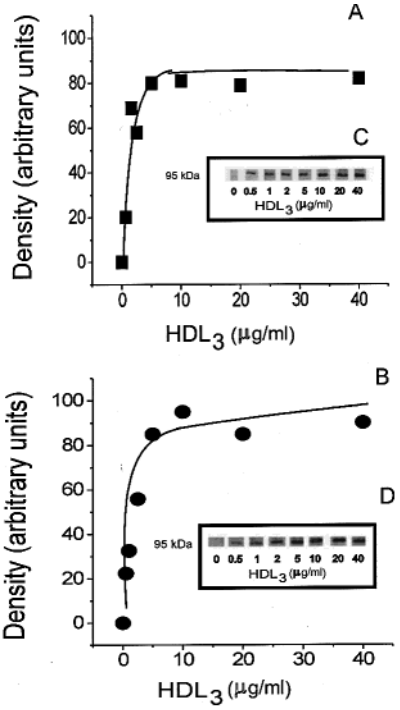

FIGURE 5: Effect of reducing conditions on HDL_3 binding with R1-HBP using a short-term modified ligand blotting protocol. Samples (200−250 μg) of the membrane proteins were boiled with an equal volume of 6.25 mM TRIS/HCl (pH 6.8)/2% SDS in the presence (panel A) or absence (panel B) of 5% (v/v) β-mercaptoethanol and subsequently processed according to the modified ligand blotting protocol (see Materials and Methods). The strips were scanned, and the points and curves were generated using a SigmaGel computer program. The curves in panels C and D correspond to the data from panels A and B, respectively.

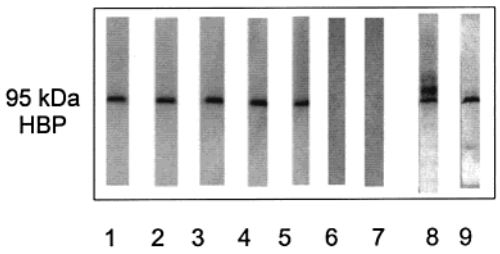

FIGURE 6: Ligand specificity of the human fetal hepatocyte plasma membrane R1-HBP utilizing a short-term modified ligand blotting protocol. Nitrocellulose strips were blocked and further incubated for 30 min at 4 °C with the following: lane 1, HDL_3 (10 μg/mL); lane 2, HDL_3 (10 μg/mL) plus LDL (20 μg/mL); lane 3, HDL_3 (10 μg/mL) plus LDL (400 μg/mL); lane 4, apoA-I (1 μg/mL); lane 5, apoA-II (1 μg/mL); lane 6, LDL (10 μg/mL). As a control, lipoprotein-free blocking buffer was used (lane 7). Lanes 8 and 9 represent the association of HDL_3 at a concentration of 10 μg/mL for 24 h in the absence (lane 8) or in the presence of 400 μg/mL LDL (lane 9).

105−115 kDa HBP's when longer incubations were performed.

Expression of the 95 kDa R1-HBP in Various Cells. Several human cell lines (HepG2, Caco-2, HeLa, PA-I, SKOV-3, fibroblasts) were used to study the tissue distribution of the 95 kDa HBP. The 95 kDa HBP was observed on all of the human cells studied as seen in Figure 7. By taking advantage of the demonstration of the 95 kDa HBP in all human studied cells and the reports about the presence of higher affinity HDL-binding sites on HepG2 cells (*11*), all further experiments were switched to a more readily available

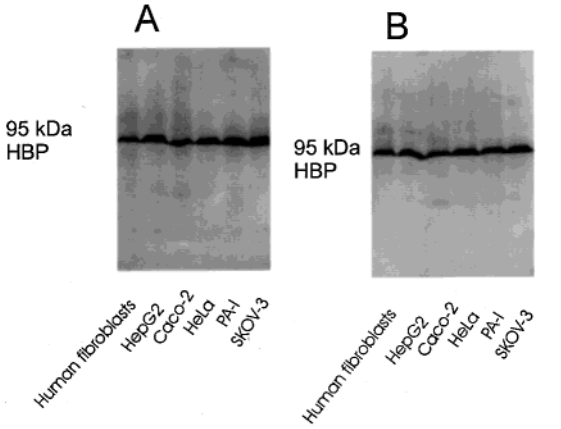

FIGURE 7: Expression of R1-HBP in various cells. Different cell lines were cultured for 48 h in serum-free media after reaching confluence. Individual plasma membrane preparations (100 μg/well) were run on a 7.5% SDS−PAGE followed by modified ligand blotting. Panel A: HDL ligand blotting (10 μg/mL); panel B: apoA-I ligand blotting (1 μg/mL).

HepG2 cell model that in addition would be independent of the quality of livers taken for hepatocyte isolation.

Effect of Tetranitromethane Modification on HDL Binding to 95 kDa R1-HBP. In good agreement with previous data, TNM-modified HDL demonstrated an upward shift of molecular mass when analyzed by native PAGE electrophoresis from 70 to 140 to 100−200 kDa (Figure 8). With increasing TNM concentrations, the amount of intact 28 kDa apoA-I gradually decreased with the appearance of multiple higher molecular mass bands when utilizing 12.5% SDS−PAGE. TNM modification abolished the ability of HDL to interact with the 95 kDa HBP (Figure 7A) while not significantly affecting the interaction with R2-HBP's.

RT-PCR Analyses of Known HDL-Binding Proteins in Various Tissues and Cells. Among recently reported HDL-binding proteins, HB-2/ALCAM has been shown to have a similar molecular mass (approximately 100 kDa) but very different binding characteristics when compared to the 95 kDa R1-HBP. We were unable to demonstrate a band corresponding to the HB-2/ALCAM protein when utilizing either short- or long-term incubations of HDL with plasma membrane samples, suggesting that HB-2/ALCAM is not expressed in fetal hepatocytes. To further address the question about HB-2/ALCAM expression in human fetal hepatocytes, RT-PCR studies were performed using total RNA preparations from human fetal hepatocytes, human fetal liver, human adult liver, and adult rat liver as well as HepG2 and McA-RH7777 cell lines. The results of the semiquantitative RT-PCR determination of HB-2, its human homologue ALCAM, CLA-1, and HBP are shown in Figure 9. Strong signals for HBP were observed for all of the samples tested. CLA-1 was expressed predominantly in rat liver, human fetal hepatocytes, and human fetal liver. A lower expression was observed in McA-RH7777 and HepG2 cell lines and adult human liver. No signals for either HB-2 or ALCAM were observed in human fetal hepatocytes. However, very strong signals for both HB-2 and ALCAM were demonstrated in adult human liver, McA-RH7777 cells, and adult rat liver. In HepG2 cells and human fetal liver, weak ALCAM but no HB-2 expression was observed. In contrast to adult liver or cultured HepG2 cells, fetal human hepatocytes demonstrate no apparent expression of HB-2/ALCAM by RT-PCR.

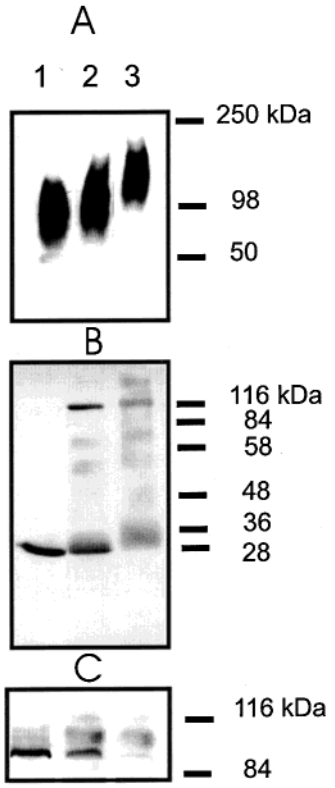

FIGURE 8: Effect of tetranitromethane on HDL_3 and apoA-I mobility and HDL_3 binding to HepG2 plasma membrane proteins. Control and TNM-treated HDL_3 samples were run on a native 4−20% Tris−glycine gel (panel A) and on a 12.5% SDS−PAGE gel (panel B). The mobilities of HDL and apoA-I were evaluated by Western blot analysis using an anti-apoA-I antibody. In panel C, HepG2 plasma membrane samples were run on a 7.5% SDS−PAGE gel followed by a modified ligand blot analysis with HDL and TNM-treated HDL_3. Lane 1, control HDL_3; lane 2, HDL_3 treated with 1 mM TNM; lane 3, HDL_3 treated with 3 mM TNM.

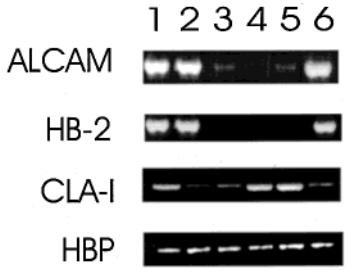

FIGURE 9: RT-PCR analysis of HDL-binding proteins in various tissues and cells. The proteins to which probe sets were generated are shown on the left side of the panel. Lane 1, adult rat liver; lane 2, McA-RH7777; lane 3, HepG2; lane 4, fetal human hepatocytes; lane 5, fetal human liver; lane 6, adult human liver.

Since fetal hepatocytes demonstrate a 95 kDa R1-HBP but do not express HB-2/ALCAM by RT-PCR, this indicates that these are two distinct HDL-binding proteins.

Localization of the 95 kDa HBP. To determine the cellular localization of the 95 kDa HBP, HepG2 cells were used. Trypsin-treated HepG2 cells or control cells (untreated cells) were used for preparation of a crude membrane fraction and cellular cytosol. As seen in Figure 10, trypsin treatment of cells eliminated approximately 70% of the 95 kDa HBP binding activity residing membrane preparation (Figure 10). The 95 kDa HBP was not detected in the cell cytosol of either trypsin-treated or untreated cells. The cytosolic protein β-actin was unaffected by trypsin treatment. These data

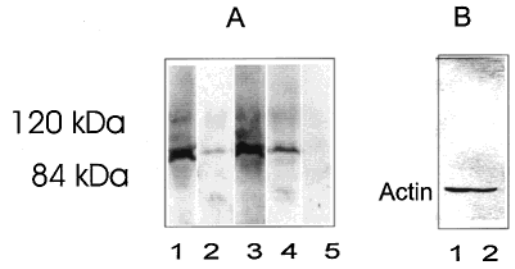

FIGURE 10: Effect of trypsin on HDL binding to the 95 kDa HDL-binding protein in HepG2 cells. (Panel A) HDL−ligand blotting: lane 1, membrane preparation from untreated cells; lane 2, membrane preparation from trypsin-treated cells; lane 3, untreated cells; lane 4, trypsin-treated cells; lane 5, cytosol from untreated cells. (Panel B) Anti-β-actin Western blotting: lane 1, cytosol from untreated cells; lane 2, cytosol from trypsin-treated cells.

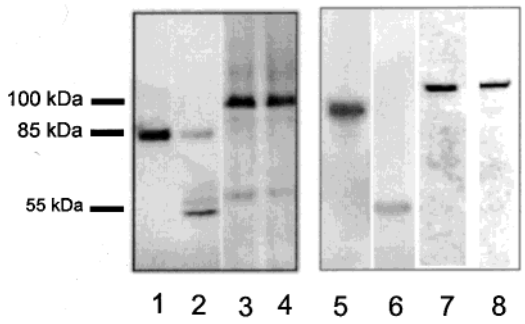

FIGURE 11: Effect of deglycosylation on SR-BI, ALCAM/HB-2, and R1-HBP activity in HepG2 cells. Western blot detection of SR-BI (CLA-1) in control extract (lane 1) and in glycosidase-treated extract (lane 2); ligand blot detection of HDL-binding protein in control extract (lane 3) and in glycosidase-treated extract (lane 4); Western blot detection of ALCAM/HB-2 in control extract (lane 5) and in glycosidase-treated extract (lane 6); Western blot detection of Gp96/GRP94 in control extract (lane 7) and in glycosidase-treated extract (lane 8).

suggest that at least 70% of the 95 kDa HBP resides on the cell surface.

Effect of Membrane Preparation Deglycosylation on the 95 kDa R1-HBP, Gp96/GRP94, HB-2/ALCAM, and SR-BI/CLA-1 HDL-Binding Proteins. At least two other HDL-binding proteins, HB-2/ALCAM and SR-BI, have been reported to be extensively glycosylated, having approximately 55−66 kDa deglycosylated forms (*3*, *14*). Gp96/GRP94 is less extensively glycosylated with only 1−2 kDa of glycosylation. To address the potential glycosylation of the 95 kDa protein, HepG2 cell Triton X-100 membrane extracts were incubated with a mixture of endo-β-*N*-acetylglucosaminidase F, *N*-glycosidase F, and endoglycosidase H. As seen in Figure 11, this enzyme treatment does not alter HDL binding to the human 95 kDa protein. In contrast, the molecular masses of SR-BI/CLA-1 and HB-2/ALCAM are reduced to approximately 55−60 kDa. No molecular mass shift was evident for Gp96/GRP94 when utilizing anti-GRP94 Western blotting. No anti-ALCAM staining was demonstrated in the human fetal hepatocyte preparations, which were positive for anti-SR-BI and CLA-1 antibodies (data not shown).

Two-Dimensional HDL Ligand Blotting. To further distinguish GRP94 from the 95 kDa HBP, partially purified crude membrane proteins were analyzed after two-dimensional electrophoresis and gradient 4−12% SDS−PAGE. Two modifications were used in the experiment: (1) the duration of electrotransfer from the gel to membrane was extended to achieve better protein recovery; and (2) a higher concentration of HDL (50 μg/mL) was used to increase the detection sensitivity. As seen in Figure 12, two distinct areas of staining with similar molecular masses are observed on the ligand blot. However, when utilizing anti-GRP94 Western blotting, only one band is observed that corresponds to the higher molecular mass HDL-binding protein. Anti-GRP94 antibodies do not stain the lower molecular mass 95 kDa HBP (Figure 12A,B). Gradient 4−12% PAGE for the same samples demonstrates the clear separation of the 95 kDa HBP and GRP94 (Figure 12C). Moreover, when comparing ligand blotting data after 1 h and overnight transfers, HDL binding to GRP94 is only observed after the longer transfer (Figure 12C, lane 2) which increased the recovery of GRP94 as measured by anti-GRP94 Western blotting (Figure 12C, lane 4). In contrast, the 95 kDa HBP has a decreased recovery when longer transfer is used.

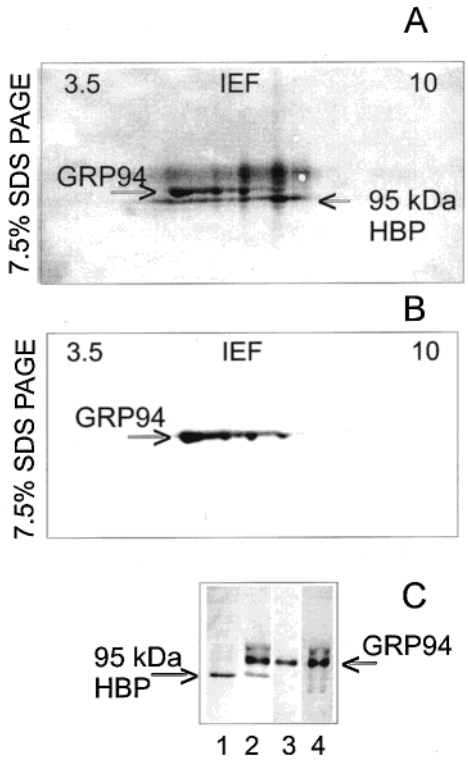

FIGURE 12: Two-dimensional and 4−12% SDS−PAGE electrophoretic analyses of the 95 kDa HBP and GRP94 in HepG2 cells. The 95 kDa protein was partially purified by preparative 7.5% SDS−PAGE, and 50 μg of this protein preparation was analyzed by two-dimensional electrophoresis and gradient 4−12% SDS−PAGE. Panel A: HDL−ligand blotting (50 μg/mL) after two-dimensional electrophoresis. Panel B: Anti-GRP94 Western blotting after two-dimensional electrophoresis. Panel C: HDL−ligand blotting (lanes 1, 2) and anti-GRP94 Western blotting (lanes 3, 4) after gradient 4−12% SDS PAGE. Lanes 1 and 3 represent results after a 1 h electrotransfer, and lanes 2 and 4 represent results after an overnight transfer.

DISCUSSION

Two families of HDL-binding sites have been reported (*10*−*12*): high-affinity sites (R1-HBS) with lower capacity and lower affinity sites (R2-HBS) with high capacity. In this report, Scatchard analysis of HDL_3-binding data identified two distinct sites on the surface of cultured human fetal hepatocytes: a high-affinity binding site with $K_{d_1} = 1.67$

μg/mL (10 nM) and $N = 13.4$ ng/mg of cell protein, and a low-affinity binding site with $K_{d_2} = 21.72$ (100 nM) μg/mL and $N = 64$ ng/mg of cell protein. K_d's from the literature for these families are in the same range; however, we observed a lower capacity for R2-HBS when compared with others (*11*). A likely reason for the difference in this study is the use of a high concentration of BSA (10−20 mg/mL) during the HDL association step, which was included in order to minimize nonspecific HDL binding. Using this same high BSA concentration, we have reported a R2-HBS with $N =$ 200 ng/mg of cell protein in rat hepatocytes (*12*).

Membrane proteins possessing HDL-binding activity have been detected by ligand blotting in the liver (*14*, *15*). For some of these proteins, the genes have been cloned, but a relationship to cholesterol metabolism has not been determined (*14*, *15*, *25*). By analyzing saturation curves reported for cells overexpressing those proteins, K_d's similar to R2-HBS have been observed (*13*−*15*). In this report, we observed two HBP's with molecular masses of 105−115 kDa whose HDL binding was determined by ligand blotting and which plateaued at 20−25 μg/mL HDL_3. Similar values have been previously reported when using specific ^{125}I-HDL_3 binding to isolated plasma membranes and cultured hepatocytes (*10*−*12*, *23*). Based on molecular mases, corresponding potential HBP's include HB-2, HBP, and GRP94. In some experiments, we have also seen weak HDL binding in the area of 55 kDa (Figure 3) and 85 kDa (Figure 7). However, it is unlikely that those bands correspond to SR-BI (CLA-1) since even when being expressed at a high level in steroidogenic cell lines such as the NCI-H295 (adrenocortical carcinoma) cell line, SR-BI demonstrated weak HDL binding when utilizing ligand blotting (*33*).

It is not surprising that HDL-binding proteins with relatively high affinity and low capacity have not yet been observed by the regular ligand blotting method. The long duration of the regular ligand blot's washing procedure exceeds the dissociation half-time of the HDL_3−R1-HBP complex by 7-fold and thus essentially eliminates all binding to the R1-HBP (*24*−*26*). By modifying the regular ligand blotting procedure to include a shorter wash step and a fixing agent, we were able to detect a 95 kDa HDL-binding protein. By assuming the amount of unbound ligand in saturation curves to be equal to the amount of added HDL in the saturation experiments, the half-saturation concentration of HDL was between 1 and 2.5 μg/mL, a range similar to R1-HBS (*10*−*12*). The 95 kDa HBP demonstrated apparently rapid association and dissociation rates (Figure 4). Both lipid-poor apolipoprotein A-I and A-II as well as HDL_3 interact with the 95 kDa HBP while LDL does not. Moreover, LDL at a concentration up to 400 μg/mL was unable to compete with HDL_3. To further evaluate the specificity of HDL binding to the 95 kDa HBP, we examined the interaction of TNM-modified HDL with the 95 kDa HBP. This modification has been reported to abolish the ability of HDL to induce translocation of intracellular cholesterol to the plasma membrane pool, and decrease specific HDL binding to the cell surface (*34*). TNM-modified HDL demonstrated both apoA-I and HDL shifts to higher molecular masses. Using concentrations of TMN which have been reported to decrease specific HDL binding to the cell surface, the modification efficiently abolished HDL binding to the 95 kDa HBP but did not alter HDL binding to the 105−115 kDa HBP's. The similar decreased efficacy of TMN-modified HDL with respect to efflux, cellular HDL_3 binding, and binding to the 95 kDa protein suggests a possible involvement of the 95 kDa protein in HDL cholesterol metabolism.

The bulk of HDL binding to the 95 kDa HBP was localized in plasma membrane preparations with virtually no activity in the cell cytosol fraction. Trypsin treatment of intact cells eliminated 70% of HDL binding to plasma membrane preparations. These data support the cell-surface localization of the 95 kDa HBP.

The potential concern that the 95 kDa R1-HBP represented the previously reported 100 kDa HB-2/ALCAM protein, the 90 kDa Gp96/GRP94, or other HDL-binding proteins was resolved by several experiments. First, while studying tissue distribution, the 95 kDa HBP was observed in all human cell lines used in this report. This observation strongly contrasted with reports of other HBP's which predominantly reside in selective cells, tissues, or cell lines. Second, treatment of plasma membrane preparations with a mixture of glycosidases did not affect HDL binding to the 95 kDa HBP while in contrast the molecular masses of CLA-1 and HB-2/ALCAM were significantly shifted to a lower value (deglycosylated form). Although the size of Gp96/GRP94 was similar to the 95 kDa HBP, two-dimensional HDL−ligand blotting and anti-GRP94 Western blotting definitively demonstrated that the proteins were different. Moreover, the experiments in Figure 12 suggest that GRP94 was not detected in ligand blotting experiments depicted in Figures 2−7 since the 1 h electro transfer resulted in an insufficient amount of GRP94 to be detected by the ligand blotting conditions used. Third, while the 95 kDa protein was expressed in human fetal hepatocytes, no expression of HB-2/ALCAM by RT-PCR was detected in human fetal hepatocytes. The sum of these data indicates that the 95 kDa protein does not correspond to previously reported HDL-binding proteins.

The role of the high-affinity binding sites still remains to be established. The recent report by Barbaras et al. (*35*) suggests the involvement of R1-HBS's with HDL endocytosis (*16*) and possibly retroendocytosis. It is possible that the ABCA-1 transporter may display binding characteristics of a R1-HBS. In cells overexpressing ABCA-I, increased ^{125}I-apoA-I binding has been observed which has been reported to be a characteristic of R1-HBS (*8*, *9*). However, ABCA-1 overexpressing cells did not show any increased ^{125}I-HDL_3 binding at a concentration of 1 μg/mL, which should predominantly detect R1-HBS (*8*). These observations suggest that R1-HBS binding is displayed by protein(s) other than ABCA-1.

In conclusion, we report the identification of a novel 95 kDa HBP that can be differentiated from other known HDL-binding proteins. The 95 kDa protein has rapid association and dissociation kinetics and binds HDL, apoA-I, and apoA-II, but not LDL. Although its role remains to be established, the 95 kDa HBP observed in this report is a possible R1-HBS because of its similar HDL-binding properties. Additional work further characterizing this protein, including its identification, will elucidate the role of the 95 kDa HBP in HDL metabolism.

ACKNOWLEDGMENT

We are very grateful to Dr. Tatiana Vlasik for providing us with monoclonal antibodies to apolipoprotein apoA-I.

REFERENCES

1. Glomset, J. A. (1968) *J. Lipid Res. 9*, 155−167.
2. Steinberg, D. (1987) *Circulation 76*, 508−514.
3. Liadaki, K. N., Liu, T., Xu, S., Ishida, B. Y., Duchateaux, P. N., Krieger, J. P., Kane, J., Krieger, M., and Zannis, V. I. (2000) *J. Biol. Chem. 275*, 21262−21271.
4. Murao, K., Terpstra, V., Green, S. R., Kondratenko, N., Steinberg, D., and Quehenberger, O. (1997) *J. Biol. Chem. 272*, 17551−17557.
5. Gu, X., Kozarsky, K., and Krieger, M. (2000) *J. Biol. Chem. 275*, 29993−30001.
6. Temel, R. E., Trigatti, B., DeMattos, R. B., Azhar, S., Krieger, M., and Williams, D. L. (1997) *Proc. Natl. Acad. Sci. U.S.A. 94*, 13600−13605.
7. Rust, S., Rosier, M., Funke, H., Real, J., Amoura, Z., Piette, J. C., Deleuze, J. F., Brewer, H. B., Duverger, N., Denefle, P., and Assmann, G. (1999) *Nat. Genet. 22*, 352−355.
8. Wang, N., Silver, D. L., Costet, P., and Tall, A. R. (2000) *J. Biol. Chem. 2000* Jul 28 [epub ahead of print].
9. Oram, J. F., Lawn, R. M., Garver, M. R., and Wade, D. P. (2000) *J. Biol. Chem. 2000* Jul 28 [epub ahead of print].
10. Morrison, J. R., McPherson, G. A., and Fidge, N. H. (1992) *J. Biol. Chem. 267*, 13205−13209.
11. Barbaras, R., Collet, X., Chap, H., and Perret, B. (1994) *Biochemistry 33*, 2335−2340.
12. Vishniakova, T. G., Bocharov, A. V., Baranova, I. N., and Repin, V. S. (1996) *Biul. Eksp. Biol. Med. 122*, 629−634.
13. McKnight, G. L., Reasoner, J., Gilbert, T., Sundquist, K. O., Hokland, B., McKernan, P. A., Champagne, J., Johnson, C. J., Bailey, M. C., and Holly, R. (1992) *J. Biol. Chem. 267*, 12131−12141.
14. Matsumoto, A., Mitchell, A., Kurata, H., Pyle, L., Kondo, K., Itakura, H., and Fidge, N. (1997) *J. Biol. Chem. 272*, 16778−16782.
15. de Crom, R. P., van Haperen, R., Willemsen, R., and van der Kamp, A. W. (1992) *Arterioscler. Thromb. 12*, 325−331.
16. Guendouzi, K., Collet, X., Perret, B., Chap, H., and Barbaras, R. (1998) *Biochemistry 37*, 14974−14980.
17. Rogler, G., Herold, G., Fahr, C., Fahr, M., Rogler, D., Reimann, F. M., and Stange, E. F. (1992) *Gastroenterology 103*, 469−480.
18. Takahashi, Y., and Smith, J. D. (2000) *Biochim. Biophys. Acta 1492*, 385−394.
19. Redgrave, T. G., Roberts, D. C. K., and West, C. E. (1975) *Anal. Biochem. 65*, 42−49.
20. Sinn, H. J., Schrenk, H. H., Friedrich, E. A., Via, D. P., and Dresel, H. A. (1988) *Anal. Biochem. 170*, 186−192.
21. Berry, M. N., and Friend, D. S. (1969) *J. Cell Biol. 43*, 506−520.
22. Seglen, P. O. (1976) *Methods Cell Biol. 13*, 29−83.
23. Bocharov, A. V., Huang, W., Vishniakova, T. G., Zaitseva, E. V., Frolova, E. G., Rampal, P., and Bertolotti, R. (1995) *Metabolism 44*, 730−738.
24. Bradford, M. (1976) *Anal. Biochem. 72*, 248−256.
25. de Crom, R. P., van Haperen, R., Willemsen, R., and van der Kamp, A. W. (1992) *Arterioscler. Thromb. 12*, 325−331.
26. Laemmli, U. K., Molbert, E., Showe, M., and Kellenberger, E. (1970) *J. Mol. Biol. 49*, 99−113.
27. O'Farrell, P. H. (1975) *J. Biol. Chem. 250*, 4007−4021.
28. Brinton, E. A., Oram, J. F., Chen, C.-H., Albers, J. J., and Bierman, E. L. (1986) *J. Biol. Chem. 261*, 495−503.
29. Bowen, M. A., Patel, D. D., Li, X., Modrell, B., Malacko, A. R., Wang, W. C., Marquardt, H., Neubauer, M., Pesando, J. M., and Francke, U. (1995) *J. Exp. Med. 181*, 2213−2220.
30. Calvo, D., and Vega, M. A. (1993) *J. Biol. Chem. 268*, 18929−18935.
31. Scatchard, G. (1949) *Ann. N.Y. Acad. Sci. 51*, 660−672.
32. Acton, S. L., Scherer, P. E., Lodish, H. F., and Krieger, M. (1994) *J. Biol. Chem. 269*, 21003−21009.
33. Martin, G., Pilon, A., Albert, C., Valle, M., Hum, D. W., Fruchart, J. C., Najib, J., Clavey, V., and Staels, B. (1999) *Eur. J. Biochem. 261*, 481−491.
34. Brinton, E. A., Oram, J. F., Chen, C. H., Albers, J. J., and Bierman, E. L. (1986) *J. Biol. Chem. 261*, 495−503.
35. Guendouzi, K., Collet, X., Perret, B., Chap, H., and Barbaras, R. (1998) *Biochemistry 37*, 14974−14980.

BI001503K